Materials Letters 168 (2016) 90–94

Contents lists available at ScienceDirect

Materials Letters

journal homepage: www.elsevier.com/locate/matlet

Growth of α-$FeSi_2$ nanocrystals on si(100) with Au catalyst

I.A. Tarasov [a,b,*], I.A. Yakovlev [a,b], M.S. Molokeev [b,c], M.V Rautskii [b], I.V. Nemtsev [d], S.N. Varnakov [a,b], S.G. Ovchinnikov [a,b]

[a] Siberian State Aerospace University, 31 Krasnoyarsky Rabochiy Av., Krasnoyarsk 660014, Russia
[b] Kirensky Institute of Physics, Russian Academy of Sciences, Akademgorodok 50, bld. 38, Krasnoyarsk 660036, Russia
[c] Far Eastern State Transport University, Serysheva str. 47, Khabarovsk 680021, Russia
[d] Krasnoyarsk Scientific Centre, Russian Academy of Sciences, Akademgorodok 50, Krasnoyarsk 660036, Russia

ARTICLE INFO

Article history:
Received 5 November 2015
Received in revised form
4 January 2016
Accepted 7 January 2016
Available online 8 January 2016

Keywords:
Nanomaterials
Molecular beam epitaxy
α-$FeSi_2$
Electrode

ABSTRACT

Self-organized α-$FeSi_2$ nanocrystals on (100) silicon substrate were synthesized by molecular beam epitaxy with Au catalyst. The microstructure and basic orientation relationship between the silicide nanocrystals and silicon substrate were analyzed in detail. α-$FeSi_2$ nanocrystals appeared to be inclined trapezoid and rectangular nanoplates, polyhedral nanobars and pyramid-like ones, aligned along $<011>$ directions on (100) silicon substrate with the length up to 1.5 μm, width ranging between 80 and 500 nm and thickness from 30 to 170 nm. As has been proposed metallic iron silicide may be used for manufacturing electric contacts on silicon. A current–voltage characteristic of the structure was measured at room temperature and showed good linearity.

1. Introduction

Iron silicides are under intensive investigations now due to their compatibility with silicon technology, economic benefits and abundance in the Earth crust [1,2]. Reducing dimension and sizes of such materials for further application in spintronics and photonics has a great potential [3,4]. For instance, it has been shown that embedding nanoparticles of semiconducting iron disilicide in a silicon matrix results in the enhancement of IR photoluminescence in comparison with ß-$FeSi_2$ thin film [5,6]. However, the intensity of room temperature IR luminescence is not as high as commercially available analogues [5]. In turn, self-assembled ß-$FeSi_2$ single-crystalline nanowires grown on silicon substrate could improve it even more [3]. Nevertheless, there are a few reports concerning their growth [3,7,8] that is possibly caused by the poor orientation relationship (OR) between ß-$FeSi_2$ and silicon. The means to achieve such Si-ß heterostructures may be by utilizing precursors. These precursors can serve other disilicides phases, α- or γ-$FeSi_2$, having a better OR with silicon [9]. To date, the forming of epitaxial α-$FeSi_2$ thin film via pulsed laser deposition [10], the annealing of prior deposited Fe film [11,12], ion implantation [13], polycrystalline film via facing target radio-frequency magnetron sputtering method [14], and subsequent Fe deposited layer annealing [15] were reported. Self-assembled α-$FeSi_2$ nanocrystals were synthesized on Si(100) and Si(111) surfaces by ion implantation [9], solid-phase epitaxy [16], and microwave plasma assisted chemical vapor deposition [17].

In this report we discuss a new approach to form self-assembled α-$FeSi_2$ nanocrystals grown on Si(100) by molecular beam epitaxy (MBE) with Au catalyst. We also explore the probable employment of the obtained crystals as the electrode to Si substrate.

2. Experiment

The α-$FeSi_2$ nanocrystals were formed on 1°- miscut vicinal p-Si(100) substrate ($\rho \sim 5$–$10\ \Omega$ cm) at 870 K by MBE in ultrahigh vacuum condition (UHV) in Angara chamber [18]. Prior to growth, Si substrate was chemically cleaned by the technique described [19]. Si substrate was exposed to gradual thermal treatment for 3 h to 650 °C at rate of 4 °C/min in UHV (base pressure 6.5×10^{-8} Pa). In order to obtain an atomically clean silicon surface the wafer was flashed at 850–900 °C until well-ordered (2×1) reconstruction appeared in the reflection high-energy electron diffraction pattern. After the specimen was cooled down to room temperature Au layer (1 nm) was evaporated from Knudsen effusion cell onto substrate surface at rate 0.25 nm/min. Then the substrate temperature was increased to 840 °C and Fe and Si were deposited simultaneously with the growth rates of 0.1 and 0.34 nm/min during 60 min. The ex situ determination of the morphology,

* Corresponding author at: Kirensky Institute of Physics, Russian Academy of Sciences, Akademgorodok 50, bld. 38, Krasnoyarsk 660036, Russia.
E-mail address: tia@iph.krasn.ru (I.A. Tarasov).

http://dx.doi.org/10.1016/j.matlet.2016.01.033
0167-577X/

phase composition of the sample was performed by scanning electron microscopy (SEM) on a Hitachi S-5500 microscope and X-ray diffraction (XRD) analysis on a D8 ADVANCE powder diffractometer (CuKα radiation, Ni filter) with a VANTEC linear detector.

3. Results and discussions

The SEM images of the sample are shown in Fig. 1. Codeposition of Fe and Si onto a silicon substrate with Au catalyst resulted in the growth of nanocrystals with the variety of the morphology. Several types of nanocrystals can be marked out. The first one are the rectangular nanoplates lying towards <010> and <011> (Fig. 1b) with the length, width and thickness about 400–800 nm, 300–400 nm and 30-70 nm, respectively. The second one are the trapezoid nanoplates inclined by ~22° relative to <100> direction and placed along <011> direction (Fig. 1c and d). The inherent sizes are almost the same for each trapezoid (height 200 nm, width 500 nm and thickness 30 nm). The third type are the polyhedral nanobars (Fig. 1b and c) aligning along <011> direction with the length up to 1.5 μm, width ranging between 100–200 nm, thickness about 50–110 nm. Habitus of the forth type is pyramid-like with length of the edges and the thickness varied from 80 to 300 nm and from 16 to 170 nm, respectively. Apart from crystallites denoted above another type exists, which have greater sizes (Fig. 1d) and possess a form of coalesced truncated pyramids. The height of them reaches 550 nm, the edges length ranging from 700 nm to 1 μm. It is easily observed that some crystallites grew on the surfaces of other crystallites (Fig. 1d) with a variety of growth direction.

The result of the sample XRD analysis is shown in Fig. 2. All

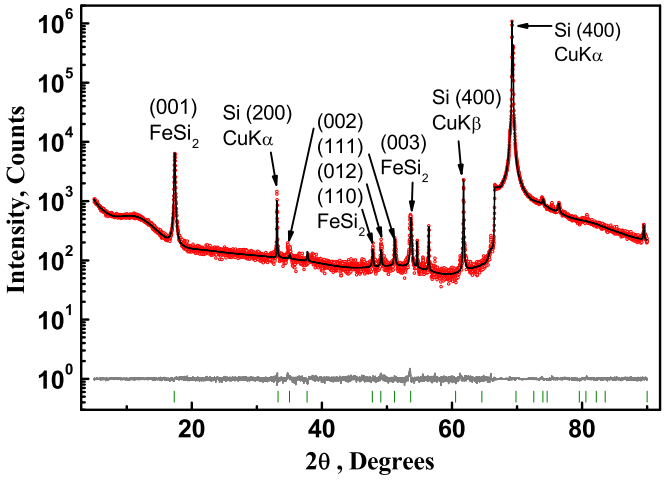

Fig. 2. Differential X-ray diffraction pattern of α-$FeSi_2$ nanocrystals on Si(100) substrate.

reflections peaks not belonging to Si(100) were successfully identified by tetragonal phase α-$FeSi_2$ [20] with the lattice constants *a*, *b*=2.6914(4) Å, *c*=5.1205(4) Å. The XRD pattern has only four unique α-$FeSi_2$ strong diffraction peaks besides several peaks from Si substrate, which are (001), (111), (012) and (110). Moreover, according to the α-$FeSi_2$ powder intensities ratios [15] the larger intensity of α(001) and α(111) peaks reveals that most of crystallites are oriented with these planes on Si(100).

Since the majority of crystallites are rectangular and pyramid-like (Fig. 1a) they are expected to have basic orientation α(001)||Si(100), α(111)||Si(100). The crystallites with the basic orientation α(001) should probably have a form of plates. Then it can be readily

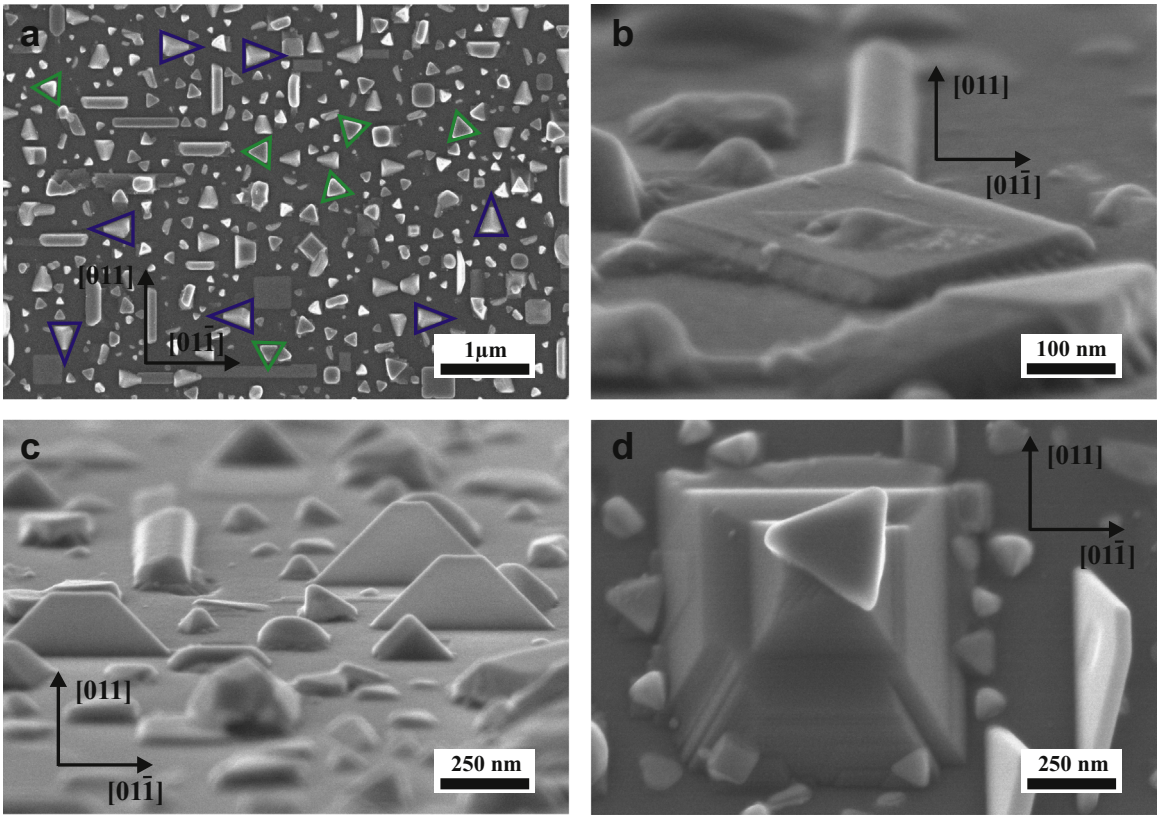

Fig. 1. SEM images of α-$FeSi_2$ nanocrystals (a) large scale view of the sample (b) magnified view of typical rectangular nanoplate, (c) trapezoid nanoplate, polyhedral nanobar and pyramid-like crystallites under tilting angle 13° away from the substrate plane (d) magnified view of truncated pyramid (sample tilting is 32°). (For interpretation of the references to color in this figure, the reader is referred to the web version of this article.)

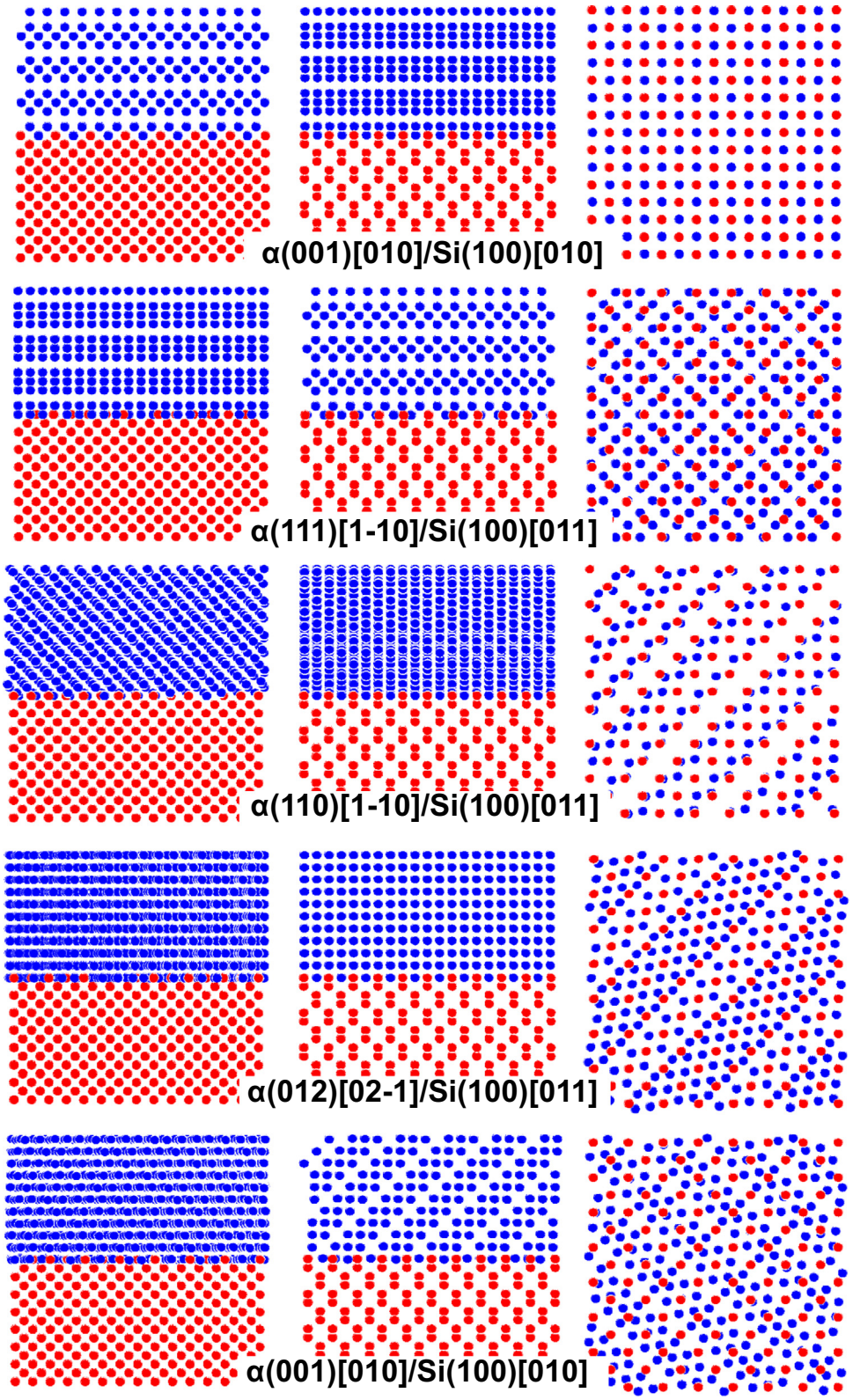

Fig. 3. Schematic drawing of interface structure for all suggested epitaxy orientation. first row refers to α(001)[010]||Si(100)[010], second – α(001)[010]||Si(100)[011], third – α(111)[1-10]||Si(100)[011], fourth – α(110) [1-10]||Si(100)[011] and fifth – α(012)[02–1]||Si(100)[011]. First column corresponds to view along $[010]^{Si}$ direction, second – $[0–11]^{Si}$ and third – $[100]^{Si}$.

seen (Fig. 1a and b) that rectangular nanoplates align along two different direction ($<010>$ and $<011>$) which means they have following OR α(001)[010]||Si(100)[010], α(001)[010]||Si(100)[011]. However, among pyramid-like crystallites it is possible to mark out two different types, one with edges having nearly the same length (Fig. 1a green triangles) and the other with the two equaled edges 1.52 times greater than the third, which the same as the ratio between the sides formed by α(111) plane in the α-$FeSi_2$ unite cell (Fig. 1a blue triangles). While the first type does not have a definite orientation direction, the second one aligns along only

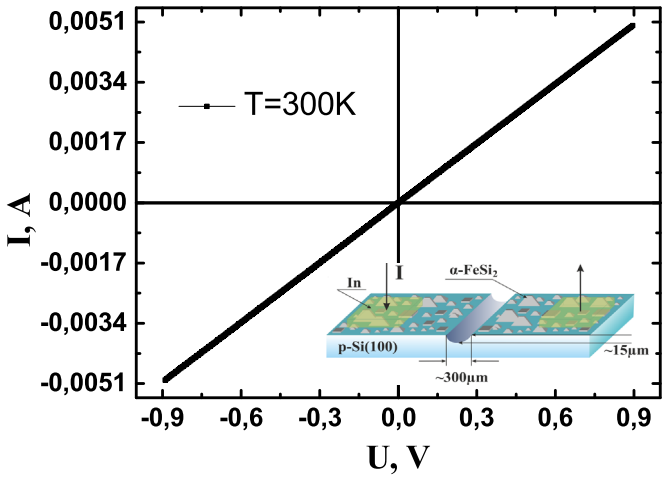

Fig. 4. Current–voltage characteristics α-$FeSi_2$ nanocrystals/p-Si(100) structure.

$<011>$. On this view the epitaxial relationship of pyramid-like crystallites, depicted as blue triangles, is α(111)[1-10]‖Si(100)[011]. The α(110)‖Si(100) crystallites probably oriented along $<011>$ direction of the silicon substrate and have the nanobar form. The most suitable direction of α(110) plane for the silicide growth is [1–10] since, as in the case of α(111) plane, silicide atomic rows coincide with silicon ones (Fig. 3). According to the XRD pattern the least volume of crystallites has to be due to a α(012)‖Si(100) orientation. This type of crystallites could grow on other α-$FeSi_2$ lumps. To presume which type of orientation the other crystallites have is difficult. The XRD pattern did not depict any other strong diffraction peaks, which could refer to these orientations of crystallites. One can assume the possible reason for such XRD pattern appearance is that the crystallites mentioned do not have any parallel to Si(100) plane or amount of such orientation is very small to give notable diffraction peaks. Such a situation could appear in the case of endotaxy [21], where the crystallites growth occurs in silicon matrix with coherent interfaces surrounding the precipitate.

Apart from these questions the role of gold catalyst on formation of a-$FeSi_2$ nanocrystals remains unclear. To clarify this issue chemical surface analysis was performed by energy-dispersive X-ray spectroscopy (EDS) on Hitachi TM-3000 microscope. The analysis revealed that the gold is uniformly distributed on the sample. However from the EDS images obtained (not showed here) it is still unclear whether the gold is on top or underneath the islands. We believe that on initial stages of the growth the silicide nanocrystals formed according to Vapor-Liquid-Crystal mechanism like in case of nanowires growth [22]. It is known that the effect of nanowires growth activation by the catalyst particles consists in the fact that growth on the surface under a droplet proceeds much faster than on a non-activated surface [23]. Here, the transition of material from vapor to liquid takes place, and as a result the solution becomes supersaturated and crystallizes on the surface under a droplet. However under certain conditions the lateral growth can be faster than the vertical growth [22,23]. The physical cause of the lateral growth initiation is a decrease in the diffusive flux from the substrate surface to the nanocrystal top, an increase in supersaturation on the side faces, and, consequently, an increase in the probability of the islands nucleation. As a consequence, a rough film of the material is formed on the surface and catalyst droplets are overgrown [22]. Hence, further work is needed to clarify the issues mentioned above.

Using the PTClab software, the interface structure of the observed on XRD pattern planes parallel to silicon surface Si(100) was calculated (Fig. 3). This calculation does not pretend to describe the real interface structure in detail and is intended to visualize a possible atomic arrangement. The calculation has been done taking into account the thermal expansion of α-$FeSi_2$ [24] and Si at the synthesis temperature.

It is clearly observed that only the α(001)[010]‖Si(100)[010] and α(111)[1-10]‖Si(100)[011] ORs have good epitaxial alignment. All three views of these α-$FeSi_2$/Si interfaces indicate a good match between silicides and silicon planes. In both cases α-$FeSi_2$ {110} and {102} planes are parallel to Si{110}. For the α(110) [1-10]‖Si (100)[011] OR one can observe only one direction when two planes, α(012) and Si(011), with the same interplanar spacing are aligned. C. Detavernier et al. [15] carried out comprehensive research of the α-$FeSi_2$ and NiSi thin film texture on Si(001) substrate. According to this work, except for epitaxial arrangement and random texture, new type of preferential orientation was observed in such structures, which was named 'axiotaxy'. In contrast to epitaxy, which is characterized by good matching within the plane of the interface, axiotaxy involves the alignment of planes across the interface [15]. Thus, the α(110) [1-10]‖Si(100) [011] crystallites, in terms of epitaxy, axiotaxy and 'random' structure crystallites can be assigned as having axiotaxy growth mode. To estimate atomic arrangement of the α(012)/Si(100) interface the OR α(012)[02–1]/Si(100)[011] was chosen as the most favorable. It can be readily seen this OR and the α(001)[010]‖Si (100)[011] one have the worst atomic arrangement. Probably the XRD peak for these planes appeared due to endotaxially grown crystallites [21] where a better atomic arrangement between planes inclined to the Si(100) one could take place.

As has been noticed [17] the α-$FeSi_2$ may be used for manufacturing electrical contacts on silicon. We carried out measurement of *I–V* characteristics of α-$FeSi_2^{crystallite}$/n-Si(100) structure. The metallic type electronic band structure of the α-$FeSi_2$ has been recently obtained in the ab initio band structure calculations within the density functional theory [25]. The device with a gap (Fig. 4 inset) was prepared to prevent possible current through the surface layer. The good linearity of *I–V* curve in Fig. 4 under -1 to +1 V bias indicated that the contact between α-$FeSi_2$ crystallites and silicon substrate had good ohmic characteristics.

4. Conclusions

In summary the growth of α-$FeSi_2$ nanocrystals on Si(100) by molecular beam epitaxy with Au catalyst is reported for the first time. The possible atomic arrangement of α/Si interfaces and the capability of utilization of α-$FeSi_2$ nanocrystals as electrical contacts to Si were explored. In this work 1°– miscut vicinal p-Si(100) substrate without an epitaxial buffer silicon layer was used, that along with the substrate temperature, the gold droplets size and their distribution, the rates material deposition could affect initiation of some type crystallite growth. We believe adjusting these parameters could be possible to synthesize only one type of the crystallites with definite sizes that would encourage application of α-$FeSi_2$ in nanoelectronics and microelectronics.

Acknowledgments

The work was supported by the Program of the President of the Russian Federation for the support of leading scientific schools (Scientific School 2886.2014.2), The Russian Foundation for Basic Research (RFBR) (Grants no. 13-02-01265), State Contract no. 02. G25.31.0043 and State Task no. 16.663.2014К).

References

[1] R. Amatya, R.J. Ram, Trend for thermoelectric materials and their earth abundance, J. Electron. Mater. 41 (2012) 1011–1019, http://dx.doi.org/10.1007/s11664-011-1839-y.

[2] E.G. Michel, Epitaxial iron silicides: geometry, electronic structure and applications, Appl. Surf. Sci. 117- 118 (1997) 294–302, http://dx.doi.org/10.1016/S0169-4332(97)80097-9.

[3] S.-W. Hung, P.-H. Yeh, L.-W. Chu, C.-D. Chen, L.-J. Chou, Y.-J. Wu, et al., Direct growth of β-$FeSi_2$ nanowires with infrared emission, ferromagnetism at room temperature and high magnetoresistance via a spontaneous chemical reaction method, J. Mater. Chem. 21 (2011) 5704, http://dx.doi.org/10.1039/c1jm10232j.

[4] M. Hilse, J. Herfort, B. Jenichen, A. Trampert, M. Hanke, P. Schaaf, et al., GaAs–Fe_3Si Core–Shell nanowires: nanobar magnets, Nano Lett. 13 (2013) 6203–6209, http://dx.doi.org/10.1021/nl4035994.

[5] D.Z. Chi, Semiconducting beta-phase $FeSi_2$ for light emitting diode applications: Recent developments, challenges, and solutions, Thin Solid Films. 537 (2013) 1–22, http://dx.doi.org/10.1016/j.tsf.2013.04.020.

[6] A.S. Fedorov, A.A. Kuzubov, T.A. Kozhevnikova, N.S. Eliseeva, N.G. Galkin, S. G. Ovchinnikov, et al., Features of the structure and properties of β-$FeSi_2$ nanofilms and a β-$FeSi_2$/Si interface, JETP Lett. 95 (2012) 20–24, http://dx.doi.org/10.1134/S0021364012010055.

[7] S. Liang, R. Islam, D.J. Smith, P.A. Bennett, Phase transformation in $FeSi_2$ nanowires, J. Cryst. Growth. 295 (2006) 166–171, http://dx.doi.org/10.1016/j.jcrysgro.2006.05.076.

[8] K. Yamamoto, H. Kohno, S. Takeda, S. Ichikawa, Fabrication of iron silicide nanowires from nanowire templates, Appl. Phys. Lett. 89 (2006) 083107, http://dx.doi.org/10.1063/1.2338018.

[9] Y. Gao, G. Shao, R.S. Chen, Y.T. Chong, Q. Li, TEM study of self-assembled $FeSi_2$ nanostructures by ion beam implantation, Solid State Commun. 149 (2009) 97–100, http://dx.doi.org/10.1016/j.ssc.2008.11.002.

[10] G. Cao, D.J. Singh, X.-G. Zhang, G. Samolyuk, L. Qiao, C. Parish, et al., Ferromagnetism and nonmetallic transport of thin-film α-$FeSi_2$: a stabilized metastable material, Phys. Rev. Lett. 114 (2015) 147202, http://dx.doi.org/10.1103/PhysRevLett.114.147202.

[11] N. Jedrecy, A. Waldhauer, M. Sauvage-Simkin, R. Pinchaux, Y. Zheng, Structural characterization of epitaxial α-derived $FeSi_2$ on Si(111), Phys. Rev. B. 49 (1994) 4725–4730, http://dx.doi.org/10.1103/PhysRevB.49.4725.

[12] J. Chevrier, P. Stocker, L.T. Vinh, J.M. Gay, J. Derrien, Epitaxial growth of α-$FeSi_2$ on Si(111) at low temperature, Europhys. Lett. 22 (1993) 449–454, http://dx.doi.org/10.1209/0295-5075/22/6/009.

[13] X.W. Lin, M. Behar, J. Desimoni, H. Bernas, J. Washburn, Z. Liliental-Weber, Low-temperature ion-induced epitaxial growth of α-$FeSi_2$ and cubic $FeSi_2$ in Si, Appl. Phys. Lett. 63 (1993) 105, http://dx.doi.org/10.1063/1.109727.

[14] S.S. Pan, C. Ye, X.M. Teng, H.T. Fan, G.H. Li, Controllable growth of α- and β-$FeSi_2$ thin films on Si(100) by facing-target sputtering, Phys. Status Solidi 204 (2007) 3316–3320, http://dx.doi.org/10.1002/pssa.200622438.

[15] C. Detavernier, C. Lavoie, J. Jordan-Sweet, A.S. Özcan, Texture of tetragonal α-$FeSi_2$ films on Si(001), Phys. Rev. B. 69 (2004) 174106, http://dx.doi.org/10.1103/PhysRevB.69.174106.

[16] J.K. Tripathi, G. Markovich, I. Goldfarb, Self-ordered magnetic α-$FeSi_2$ nanostripes on Si(111), Appl. Phys. Lett. 102 (2013) 251604, http://dx.doi.org/10.1063/1.4812239.

[17] B.-X. Xu, Y. Zhang, H.-S. Zhu, D.-Z. Shen, J.-L. Wu, Fabrication and mechanism of α-$FeSi_2$ nanobars on (001) silicon wafer, Mater. Lett. 59 (2005) 833–837, http://dx.doi.org/10.1016/j.matlet.2004.10.060.

[18] S.N. Varnakov, A.A. Lepeshev, S.G. Ovchinnikov, A.S. Parshin, M.M. Korshunov, P. Nevoral, Automation of technological equipment for obtaining multilayer structures in an ultrahigh vacuum, Instrum. Exp. Tech. 47 (2004) 839–843, http://dx.doi.org/10.1023/B:INET.0000049709.08368.3e.

[19] I.A. Yakovlev, S.N. Varnakov, B.A. Belyaev, S.M. Zharkov, M.S. Molokeev, I. A. Tarasov, et al., Study of the structural and magnetic characteristics of epitaxial Fe3Si/Si(111) films, JETP Lett. 99 (2014) 527–530, http://dx.doi.org/10.1134/S0021364014090124.

[20] A. Wittmann, K.O. Burger, H. Nowotny, Untersuchungen im Dreistoff: Ni-Al-Si sowie von Mono- und Disilicidsystemen einiger Übergangsmetalle, Monatshefte Chem. 93 (1962) 674–680, http://dx.doi.org/10.1007/BF01189606.

[21] D. Das, J.C. Mahato, B. Bisi, B. Satpati, B.N. Dev, Self-organized patterns along sidewalls of iron silicide nanowires on Si(110) and their origin, Appl. Phys. Lett. 105 (2014) 191606, http://dx.doi.org/10.1063/1.4901815.

[22] V.G. Dubrovskii, G.E. Cirlin, V.M. Ustinov, Semiconductor nanowhiskers: Synthesis, properties, and applications, Semiconductors 43 (2009) 1539–1584, http://dx.doi.org/10.1134/S106378260912001X.

[23] V.G. Dubrovskii, N.V. Sibirev, G.E. Cirlin, M. Tchernycheva, J.C. Harmand, V. M. Ustinov, Shape modification of III-V nanowires: the role of nucleation on sidewalls, Phys. Rev. E 77 (2008) 031606, http://dx.doi.org/10.1103/PhysRevE.77.031606.

[24] F. Zhang, S. Saxena, Phase stability and thermal expansion property of $FeSi_2$, Scr. Mater. 54 (2006) 1375–1377, http://dx.doi.org/10.1016/j.scriptamat.2005.11.076.

[25] I. Sandalov, N. Zamkova, V. Zhandun, I. Tarasov, S. Varnakov, I. Yakovlev, et al., Effect of electron correlations on the Fe_3Si and α-$FeSi_2$ band structure and optical properties, Phys. Rev. B 92 (2015) 205129, http://dx.doi.org/10.1103/PhysRevB.92.205129.